Crystal Structure of Antithrombin in a Heparin-Bound Intermediate State[†,‡]

Daniel J. D. Johnson and James A. Huntington*

Department of Haematology, Cambridge Institute for Medical Research, Wellcome Trust/MRC Building, Hills Road, Cambridge CB2 2XY, United Kingdom

Received April 2, 2003; Revised Manuscript Received May 20, 2003

ABSTRACT: Antithrombin is activated as an inhibitor of the coagulation proteases through its specific interaction with a heparin pentasaccharide. The binding of heparin induces a global conformational change in antithrombin which results in the freeing of its reactive center loop for interaction with target proteases and a 1000-fold increase in heparin affinity. The allosteric mechanism by which the properties of antithrombin are altered by its interactions with the specific pentasaccharide sequence of heparin is of great interest to the medical and protein biochemistry communities. Heparin binding has previously been characterized as a two-step, three-state mechanism where, after an initial weak interaction, antithrombin undergoes a conformational change to its high-affinity state. Although the native and heparin-activated states have been determined through protein crystallography, the number and magnitude of conformational changes render problematic the task of determining which account for the improved heparin affinity and how the heparin binding region is linked to the expulsion of the reactive center loop. Here we present the structure of an intermediate pentasaccharide-bound conformation of antithrombin which has undergone all of the conformational changes associated with activation except loop expulsion and helix D elongation. We conclude that the basis of the high-affinity state is not improved interaction with the pentasaccharide but a lowering of the global free energy due to conformational changes elsewhere in antithrombin. We suggest a mechanism in which the role of helix D elongation is to lock antithrombin in the five-stranded fully activated conformation.

Antithrombin binds to a specific pentasaccharide sequence found on the heparan sulfates which line the endothelium of the microvasculature. This pentasaccharide sequence is also found in heparin where it was first identified as the minimal antithrombin binding sequence (*1*) and has since been chemically synthesized (*2*) and is now marketed as an antithrombotic agent (Fondaparinux). The interaction between antithrombin and the pentasaccharide has been mapped by mutagenesis (for review see ref *3*) and observed in a crystallographic structure of the complex (*4*), and the mechanism by which heparin binding accelerates the inhibition of the coagulation proteases is also well understood (for review see ref *5*). The rate of factor Xa inhibition is significantly enhanced through a heparin-induced conformational change in antithrombin, whereas efficient inhibition of thrombin requires both thrombin and antithrombin to occupy the same heparin chain. Thus, the pentasaccharide is sufficient to effect a 300-fold increase in the rate of factor Xa inhibition but only a 2-fold increase in the rate of thrombin inhibition. The distinct mechanisms are commonly referred to as the "allosteric" and "bridging" (or template) mechanisms.

The conformational change in antithrombin which results from pentasaccharide binding affects not only the rate of protease inhibition but also the affinity of antithrombin for heparin. Stopped-flow intrinsic fluorescence studies have determined that heparin binding is a two-step, three-state process where, after the formation of a weakly interacting intermediate complex ($K_d \sim 20\ \mu$M), antithrombin undergoes a conformational change to form a tight, high-affinity complex ($K_d \sim 20$ nM) (*6*) (Figure 1a). The presence of a fluorescently silent intermediate state was inferred from the hyperbolic nature of the plots of rate vs heparin concentration (while pseudo first-order in heparin). It has since been discovered that the native conformation of antithrombin is unusual among the other members of the SERPIN family of protease inhibitors (*7*). While most serpins have a fully exposed reactive center loop and a five-stranded β-sheet A, the reactive center loop of antithrombin is partially inserted into β-sheet A (*8*, *9*). The effect of heparin binding is to expel the reactive center loop from β-sheet A, thus freeing it for interaction with proteases. The secondary structure of antithrombin changes, as indicated in Figure 1b, and can be summarized as the extension of helices A and D, the formation of helix P, and the expulsion of the reactive center loop with the consequent zipping up of the gap between strands 3 and 5 of β-sheet A. In concert with the secondary structural changes in the heparin binding region is a global rearrangement of the packing of antithrombin. This can be best described as a rotation of the lower helical domain relative to the upper β-barrel domain (*10*). It has been established through the individual mutation of the four tryptophans in antithrombin that Trp225 and Trp307, located in the upper β-barrel domain, are primarily responsible for the 40% fluorescence enhancement observed upon heparin

[†] J.A.H. is funded by the NIH (R01 HL68629) and the MRC (U.K.).

[‡] Coordinates and structure factors were deposited in the Protein Data Bank under the PDB ID code of 1NQ9.

* To whom correspondence should be addressed. Tel: +44 1223 762660. Fax: +44 1223 336827. E-mail: jah52@cam.ac.uk.

10.1021/bi034524y CCC: $25.00
Published on Web 07/04/2003

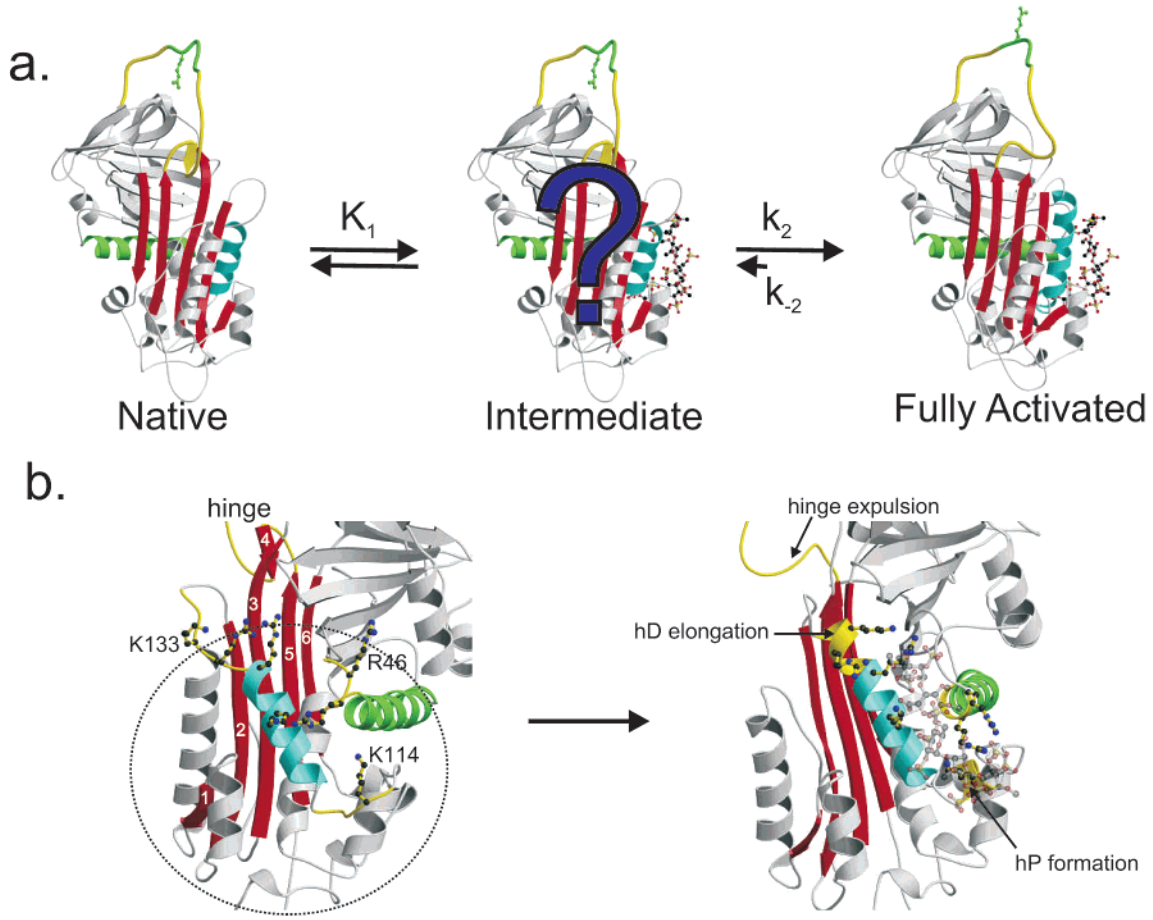

FIGURE 1: Heparin binding mechanism of antithrombin. (a) Antithrombin (ribbon diagram) interacts with heparin (ball-and-stick representation) in a two-step, three-state mechanism. The native state is in the low-activity and low-affinity conformation with its reactive center loop (yellow and green) partially inserted into the main β-sheet A (red). The specific heparin pentasaccharide interacts with antithrombin primarily via helices A (green) and D (cyan). The weak binding intermediate (center panel) undergoes a conformational change resulting in a 40% intrinsic fluorescence enhancement to create a high-affinity complex (right panel). The conformational changes result in the expulsion of the reactive center loop and contraction of β-sheet A, which frees the P1 Arg (green ball-and-stick representation) for interaction with target proteases. (b) A close-up of the heparin binding region of antithrombin reveals the nature of the heparin-induced conformational changes. Binding of the pentasaccharide (transparent ball-and-stick representation) and conversion from the native (left) to fully activated conformations (right) cause secondary and tertiary structural changes (yellow) in antithrombin, including the C-terminal elongation of helix D, the formation of helix P at the N-terminus of helix D, the ordering of the N-terminus of helix A, and the expulsion of the hinge region (s4A) from β-sheet A. These changes are accompanied by the rotation of the lower helical domain (circled) relative to the upper β-barrel domain. Heparin binding residues (R46, R47, K114, K125, K129, R131, and K133) are shown in ball-and-stick representation.

binding (*11*). The position of Trp225 directly under the inserted portion of the reactive center loop hinge suggests that it is the closing of β-sheet A to the five-stranded form which results in the high-affinity state.

Although the pentasaccharide binding site and the conformational change from native to heparin-activated antithrombin have thus been determined, fundamental questions concerning the mechanism persist. For instance, how does the conformational change in antithrombin bring about high affinity for heparin? It has been assumed for many years that the interaction interface is improved so that more favorable ionic and nonionic interactions are formed, but it is also possible that the improvement in binding derives from a lower global energy due to conformational changes elsewhere in antithrombin. Is high affinity achieved through improved interactions with heparin? Which of the many conformational changes in antithrombin are responsible for producing high heparin affinity? How is the remote binding of the pentasaccharide coupled to the expulsion of the reactive center loop? These questions lie at the heart of antithrombin allostery and are all related to the conformation of the intermediate heparin-bound state (Figure 1a). In this paper we describe the structure of an intermediate antithrombin−pentasaccharide complex which we believe represents the intermediate state and which satisfyingly answers the questions posed above.

EXPERIMENTAL PROCEDURES

Materials. The fully glycosylated α glycoform of antithrombin was derived from freshly frozen human plasma as previously described (*12*). Subsequently, antithrombin was partially deglycosylated by simultaneous treatment with neuraminidase (Sigma), β(1−4)-galactosidase (Prozyme), and β-*N*-acetylglucosaminidase (Sigma) as previously described (*13*), resulting in an α-like form with the branched mannose carbohydrate Manα1→6(Manα1→3)−Manβ→4GlcNAcβ1→4GlcNAc$_{OT}$ intact. Partial deglycosylation was performed to decrease the hydrodynamic radius of the carbohydrate, thus favoring the formation of crystal contacts. The extent of our deglycosylation produces an antithrombin molecule equiva-

lent to the recombinant α form produced by baculovirus in sf9 cells (*14*, *15*). The loss of negative charge of the sialic acid groups results in a 10-fold increase in heparin affinity with a similar change in intrinsic fluorescence but no change in basal rates of factor Xa inhibition (data not shown). The properties of the partially deglycosylated antithrombin are consistent with previous studies on recombinant α-antithrombin from baculovirus. Following purification of the partially deglycosylated material by heparin−Sepharose chromatography (Amersham), a portion of the antithrombin was converted to the latent form using the glycerol method (*16*). The high-affinity pentasaccharide (SANORG 34006) was the kind gift of Dr. Maurice Petitou, Sanofi Research, Toulouse, France. 1-Anilinonaphthalene-8-sulfonic acid (ANS)[1] was purchased from Molecular Probes, Eugene, OR, and all crystallization reagents were purchased from Hampton Research, Aliso Vlejo, CA.

Crystallization and Structure Determination. Crystals were obtained using the hanging drop method from drops containing 7.2 mg/mL antithrombin (native and latent in a 1-to-1 ratio), high-affinity pentasaccharide (1.1:1 molar excess over antithrombin), 10 mM Tris, pH 7.4, 128 mM NH_4F, 12.8% PEG 3350, 20% glycerol, and 0.35 mg/mL ANS. Data were collected at the SRS Daresbury Station 14.1 from a single crystal taken directly from the crystallization drop and flash cooled to 100 K. The data were of unusually high quality for antithrombin crystals, diffracting strongly to 2.6 Å with a mosaic spread of only 0.4, and were integrated using Mosflm and processed with Scala and Truncate from the CCP4 suite of programs (*17*) (statistics are given in Table 1). Molecular replacement using MolRep (*18*) placed one pentasaccharide-bound latent antithrombin molecule in the asymmetric unit (1e03, chain L), and solutions were found using both pentasaccharide-bound (1e03, chain I) and native (1e05, chain I) forms of antithrombin. The pentasaccharide-bound active component yielded a significantly better score (TF/sig of 21.6 vs 17.5) and was thus chosen as the solution. After maps were generated using both sets of molecular replacement solutions, it was clear that the active form of antithrombin in the crystal possessed a nativelike hinge although the heparin binding region was almost identical to the active molecule in the pentasaccharide-activated structure (supplementary figure in Supporting Information). A hybrid molecule was thus created using the N-terminus of the pentasaccharide-bound molecule (1e03, residues 42−213) and the C-terminus of the native molecule (1e05, residues 214−432) on the basis of agreement with the electron density maps. After rigid body refinement of the individual fragments, sequential rounds of rebuilding [XtalView (*19*)] and coordinate and *B*-factor refinement using CNS (*20*) resulted in a model comprising residues 5−26, 36−133, 136−398, and 401−430 for the latent molecule and residues 6−26, 39−133, 137−355, and 361−431 for the active molecule. The reflections chosen for the *R*-free set were identical to those used for other antithrombin structures (1e03, 1e04, and 1e05) (*21*) to allow for a more rigorous comparison of the resulting structures. Statistics for the final model and its refinement are given in Table 1. Figures were generated using Molscript (*22*), Bobscript (*23*), and Raster3D (*24*). Coordinates and structure factors were deposited in the Protein Data Bank under the PDB ID code of 1NQ9.

Table 1: Data Processing, Refinement, and Model (1NQ9)

crystal		
space group	$P2_1$	
cell dimensions	$a = 69.68$ Å $b = 86.76$ Å $c = 96.92$ Å $\beta = 109.54°$	
solvent content (%)	50	
data processing statistics		
wavelength (Å)	1.244 (SRS Daresbury, Station 14.1)	
resolution (Å)	24.62−2.60	2.74−2.60
total reflections	120627	14878
unique reflections	33466	4740
multiplicity	3.6	3.1
$\langle I/\sigma(I)\rangle$	6.9	1.3
$\langle I\rangle/\sigma(\langle I\rangle)$	10.7	1.9
completeness (%)	99.6	99.6
R_{merge}[a]	0.092	0.571
model		
no. of atoms modeled		
protein	6467	
water	89	
carbohydrate	112	
pentasaccharide	200	
average *B*-factor (Å^2)	49.8	
refinement statistics		
resolution (Å)	24.43−2.60	2.76−2.60
reflections in working/free set	31798/1666	5199/245
R-factor[b]/*R*-free (%)	20.9/25.0	33.8/37.2
RMSD of bonds (Å)/ angles (deg) from ideality	0.008/1.3	
Ramachandran plot: residues in		
most favored region (%)	86.8	
additionally allowed region (%)	12.1	
generously allowed region (%)	1.1	
disallowed region (%)	0	

[a] $R_{merge} = \sum_{hkl}\sum_i|I_{hkl} - \langle I_{hkl}\rangle|/\sum_{hkl}\sum_i\langle I_{hkl}\rangle$. [b] *R*-factor $= \sum_{hkl}||F_o| - |F_c||/\sum_{hkl}|F_o|$.

RESULTS

Overall Structure. A ribbon diagram of the asymmetric unit is given in Figure 2 and clearly demonstrates the presence of the heterodimer with each monomer in complex with one molecule of the pentasaccharide. The latent molecule is nearly identical to that previously solved with a Cα root mean squared deviation (RMSD) of 0.706 Å for the 411 equivalent atoms, with the apparent difference probably arising from the differences in resolution and data quality (1e03 resolution was 2.9 Å). The active component of the dimer differs by 0.847 Å for the 405 Cα atoms in common with the previously solved structure of pentasaccharide-bound active antithrombin (1e03 chain I) and 1.578 Å for the 405 Cα atoms in common with the previously solved structure of active α-antithrombin (1e05 chain I, determined to 2.6 Å resolution). Clearly, the majority of the structure of the active component in our crystal more closely resembles the previous structure of activated than that of native antithrombin. There are, however, structural elements of both native and activated antithrombin in the active component of our structure, as demonstrated in Figure 3. Figure 3a is a Cα trace of our active component colored according to RMSD with the native structure, and Figure

[1] Abbreviations: ANS, 1-anilinonaphthalene-8-sulfonic acid; TNS, 2-*p*-toluidinylnaphthalenesulfonate; RMSD, root mean squared deviation.

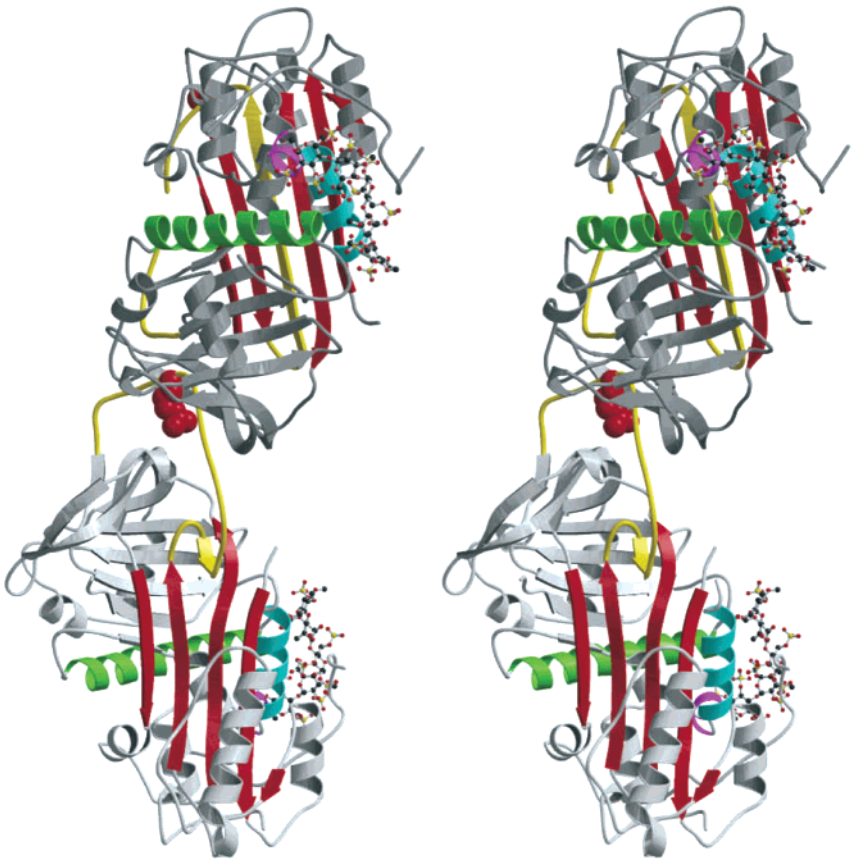

FIGURE 2: Stereo representation of the asymmetric unit. The asymmetric unit consists of the heterodimer between latent (top) and active (bottom) forms of antithrombin (colored as in Figure 1 but with helix P in magenta). Both are clearly bound to the pentasaccharide. Surprisingly, the hinge of the active component resembled the native, and not the fully activated, antithrombin structure.

3b shows the difference with the activated structure. As indicated by the overall RMSD values and illustrated in Figure 3, our active form is more similar to the pentasaccharide-bound activated structure than that of unliganded, native antithrombin. It can be said that the lower, helical domain of our active monomer has undergone the activating conformational change but that the upper, β-barrel domain has not. In fact, when the structures are overlaid (Figure 3c), it is clear that the active component in our structure is in an intermediate conformation between native and activated antithrombin.

The Hinge Region. As Figure 1 illustrates, the activation of antithrombin by heparin involves the expulsion of the hinge region of the reactive center loop from β-sheet A. β-Sheet A then closes up to the five-stranded form commonly found in the structures of native serpins [e.g., α_1-antitrypsin (*25*), PAI-1 (*26*), α_1-antichymotrypsin (*27*), and *Manduca sexta* serpin K (*28*)]. The most surprising finding in our structure was that the hinge region of the active component was in the nativelike, β-sheet-incorporated form despite having the same high-affinity pentasaccharide ligand bound. The electron density of the hinge region and parts of strands 3 and 5A is given in Figure 4a and unequivocally demonstrates the veracity of the structure. The partial insertion of the reactive center loop in the native form of antithrombin breaks the hydrogen bonds between strands 3 and 5A from the top of the sheet to the equivalent position of P8 in latent antithrombin (in which the reactive center loop is fully inserted into β-sheet A). The first hydrogen bond after the insertion point is thus between N217 and F368 in native antithrombin, with an N-to-O distance of 2.97 Å. In the intermediate structure determined here, β-sheet A has been closed up to the equivalent position of P11 in latent AT, which corresponds to residues I219 and F372 with an N-to-O distance of 3.41 Å (Figure 4a). Consequently, several water molecules have been expelled from the gap, and only one is found in the structure of the intermediate form (Figure 4a). Recent work has focused on the role that the interactions of P13 Glu plays in stabilizing the native state and in propagating the conformational change, initiated by heparin binding, from the heparin binding region to the hinge region (*29*). The interactions of the P13 Glu side chain are different in the intermediate form when compared to the native form, but they are nonetheless quite strong (Figure 4a).

The Heparin Binding Region. The electron density for the synthetic high-affinity pentasaccharide and the heparin binding region of antithrombin is of very high quality and demonstrates unequivocally that, even though the hinge region is in the nativelike, β-sheet-inserted conformation, the pentasaccharide is bound in an identical fashion to fully activated antithrombin (Figure 4b). The interactions between the intermediate form of antithrombin and the high-affinity pentasaccharide correspond with those described earlier for fully activated antithrombin (*4*). Although the side chains of Lys11, Arg46, and Lys125 cannot be fully traced into the electron density, they are clearly in position to have one or several interactions with the pentasaccharide. Similarly, in the structure of fully activated antithrombin the side chains of Arg13 and Lys125 cannot be fully traced but are in position to have one or several contacts. Therefore, the

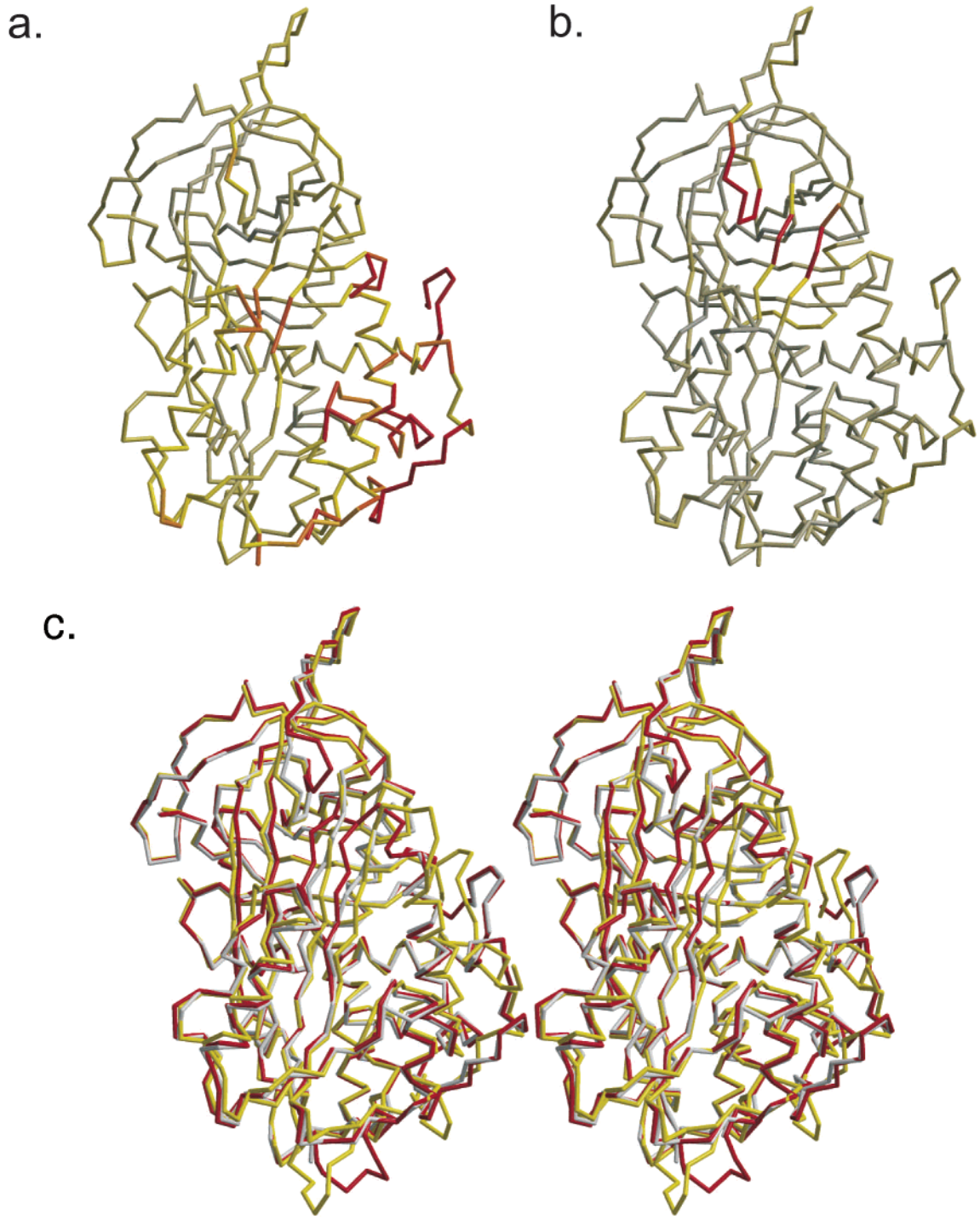

FIGURE 3: Comparison of the intermediate structure with native and fully activated structures. (a) The Cα trace of the pentasaccharide-bound intermediate, oriented roughly as in Figure 1a, colored according to the RMS deviation with native (1e05) antithrombin, from gray to yellow to orange to red for 0−3 Å RMSDs. (b) As in (a) but compared to the fully activated structure of antithrombin (1e03). (c) Stereo representation of the Cα traces of all three structures with native in yellow, intermediate in gray, and activated in red.

position of the pentasaccharide in the heparin binding site, the shape of the heparin binding site, and the interactions between the pentasaccharide and antithrombin are identical for the intermediate heparin-bound conformation and the final, activated heparin-bound conformation.

DISCUSSION

Since the simultaneous observation by two separate groups that crystallization of pure native antithrombin resulted only in crystals of a heterodimer between active and latent forms (*8*, *9*), all subsequent antithrombin structures have been obtained from crystals derived from equimolar mixtures of the two antithrombin conformers. The finding that the active molecule, representing the native form, possessed a partially inserted reactive center loop suggested that the mechanism of activation counterintuitively involved the expulsion rather than the insertion of the reactive center loop upon heparin binding. Later this was verified by fluorescence solution studies (*30*, *31*) and by the crystal structure of the antithrombin dimer complexed with a high-affinity synthetic pen-

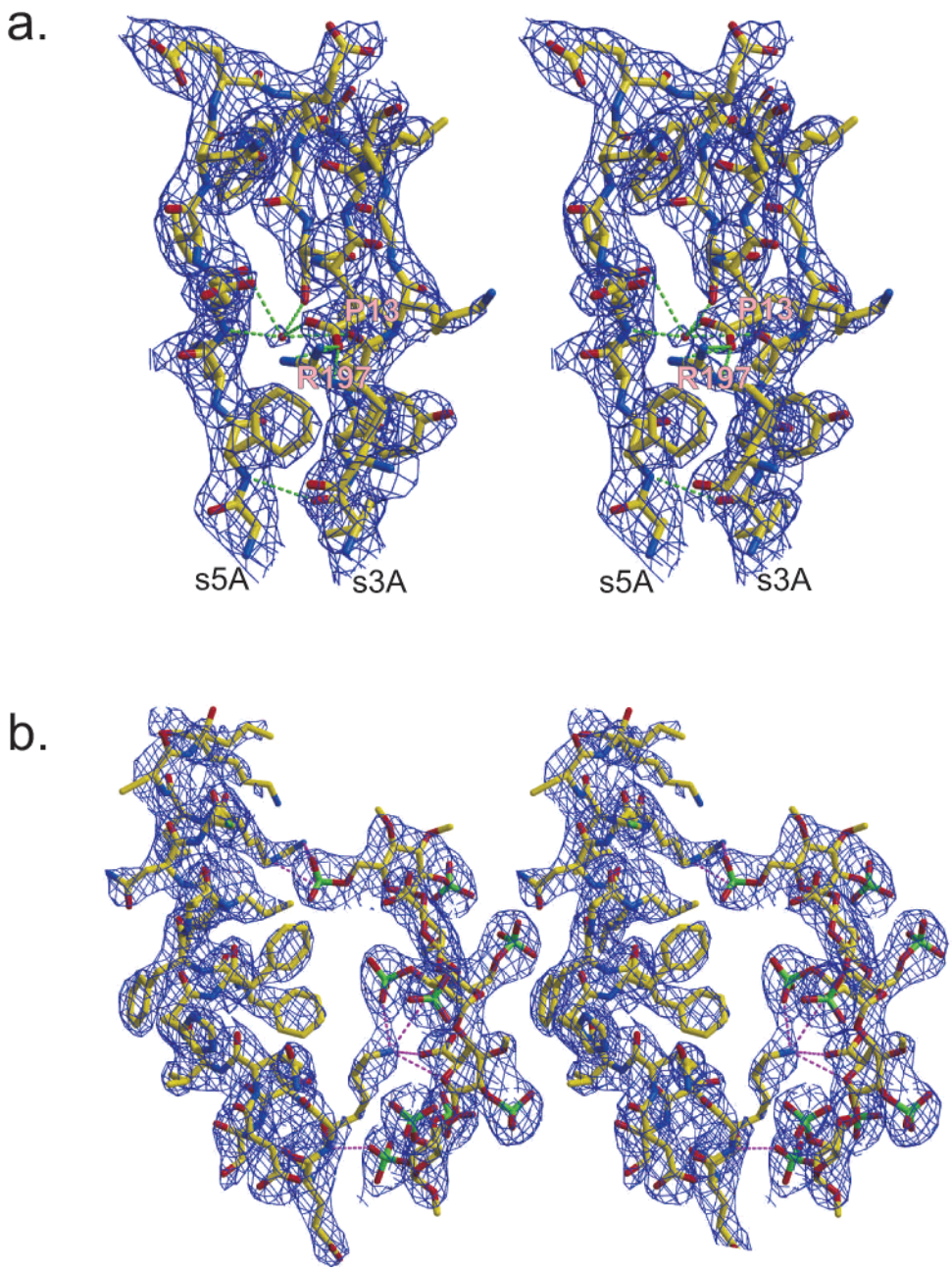

FIGURE 4: Stereo representations of the electron density in the hinge and heparin binding regions contoured at 1σ. (a) The hinge of the intermediate is inserted into β-sheet A as the fourth strand, similar to the native conformation. Unlike native, however, β-sheet A is partially contracted with the first hydrogen bond between residues I219 and F372 (dashed green line). Only one water molecule is left in the cleft between strands 3 and 5A, which is the center of a hydrogen bond network involving the side chains of Arg197 on helix F, Glu381 (P13), Thr380 (P14), and the main chains of strands 3 and 5A. (b) Electron density of helices P and D (left) and the pentasaccharide (right, with green for sulfur atoms) demonstrates an identical interaction interface with fully activated antithrombin. Hydrogen-bonding and salt-bridging interactions are shown as dashed magenta lines. The major interactions between Lys114 (middle) and Arg129 (top) with the pentasaccharide are shown. Other pentasaccharide interactions are omitted for clarity.

tasaccharide (*4*). In this paper we describe the structure of antithrombin bound to the same high-affinity pentasaccharide which has not undergone the full activating conformational change. Two questions must be addressed: (1) Does this structure represent *the* intermediate heparin-bound state? (2) Why did we not obtain the fully activated structure? That we have crystallized antithrombin bound to a heparin pentasaccharide in a conformation intermediate between the native and activated forms is clear from the experimental data and would suggest that our structure represents a conformational intermediate on the pathway to full activation. Heparin binding is, however, a dynamic process, and protein structures obtained from crystals are conformationally frozen by the intermolecular contacts within the crystal. It is thus difficult to state conclusively that the antithrombin form obtained in our crystal represents *the* kinetic intermediate identified from intrinsic fluorescence stopped-flow experiments. All that is known about the kinetic intermediate is that it is bound to heparin and that it is fluorescently silent, so the claim that our structure is the kinetic intermediate must at least satisfy these two points. Clearly, the intermediate structure presented here is bound to heparin, as demonstrated in Figure 4b. One feature of our structure is that the "top" of the molecule is in a nativelike state, and since the

two tryptophans (225 and 307) which account for the vast majority of the intrinsic fluorescence enhancement are located in the top of the molecule, their quantum yields should be similar to those found in the native conformation. Thus it is possible that the structure of the pentasaccharide-bound active component obtained from our crystal represents the kinetic intermediate between native and heparin-activated antithrombins. But why did this intermediate form crystallize under our conditions? The only other deposited crystal structure of antithrombin bound to a heparin analogue was crystallized under similar conditions with the same high-affinity pentasaccharide. Again, this is a difficult question to answer satisfactorily without the determination of a string of structures obtained from systematically altered conditions. We would suggest that whatever the change in condition it would need to either alter the equilibrium position between the intermediate and the fully activated heparin bound states or increase the time of crystallization sufficiently such that a minor solution conformer could preferentially crystallize out. Our crystallization conditions might have had both effects. Whereas our crystals were obtained from drops containing physiological pH and ionic strength (pH 7.4 and $I \sim 0.15$), the previous crystals were obtained at pH 7 and low ionic strength ($\sim$0.03). Since the strength of heparin binding by antithrombin is improved at lower pH and ionic strength, we would expect that the equilibrium position in our drops would be slightly more toward the intermediate state. In addition, the previous crystals were obtained by the batch method, which encourages instantaneous crystallization, whereas our crystals were obtained over a period of weeks from drops which were undergoing slow dehydration using the hanging drop method. It is also possible that partial deglycosylation of α-antithrombin also played a role in determining which form crystallized; however, all of the carbohydrate up through the branched mannose is still intact, and removal of the sialic acid groups results in 10-fold greater affinity for heparin, not a reduction. Other differences in conditions such as the presence of glycerol and ANS may also have an effect of the equilibrium between the intermediate and the fully activated states; however, the magnitude of the intrinsic fluorescence enhancement is unaltered in glycerol (data not shown), and the closely related fluorophore TNS does not affect the heparin affinity of antithrombin (*11*). In addition, we have recently solved a related structure of the physiological pentasaccharide bound to fully glycosylated α-antithrombin, which crystallized under similar conditions but in the absence of glycerol and ANS. Although the structure was only solved to 3.5 Å resolution, it too clearly possessed a nativelike hinge region (data not shown). It may thus not be possible to determine which of the many differences are responsible for the crystallization of the partially activated form we found in our crystals, but it is clear that in solution an equilibrium exists between the fully active and the intermediate form presented here. Since the magnitude of the intrinsic fluorescence enhancement upon heparin binding is a function of the ratio between the fluorescently silent intermediate and the fully activated states, one would expect that the fluorescence enhancement would be related to the strength of binding. This however is not the case. Although the total fluorescence enhancement varies between experiments and with different antithrombin variants, the total fluorescence enhancement is independent of strength of interaction provided that the minimal pentasaccharide sequence is present. Thus there is no significant difference between the ratio of the intermediate form and the fully activated form at saturation provided that the minimal binding pentasaccharide is present. This implies that in the presence of the pentasaccharide the ratio is at least 1:9 and that improvement in affinity due to either lowering ionic strength, the addition of nonreducing end heparin residues, or the addition of sulfate groups or O-methylation will not appreciably affect the ratio.

It has long been believed that the two steps of heparin binding were best described by a weak interaction followed by a conformational change to a high-affinity state. It appears from this structure that both steps involve conformational change. In fact, from the RMSDs and figures colored according to the RMSDs it is evident that there is more conformational change going from native to intermediate than from intermediate to fully active. To better visualize the contribution of conformational change to each of the two steps, a movie of pentasaccharide binding was created using the coordinates of the three structures, native, intermediate, and fully activated, and a series of intervening coordinates generated by the Morph server (http://molbio.info.nih.gov/structbio/indie_morph.html). The result is a compelling demonstration of the entire heparin binding mechanism of antithrombin (available as a supplementary video in Supporting Information). All of the conformational changes, save helix D elongation and the expulsion of the hinge from β-sheet A, have already occurred in the intermediate structure. These include the rotation of helix D, the formation of helix P, the bending of helix A, the closing of the bottom of β-sheet A, the rotation of helix F, and the movement of the upper β-barrel and the lower helical domains relative to one another. The paucity of conformational change in the second step is fortuitous. Instead of having to determine which of a myriad of conformational changes result in the high-affinity state, the problem is reduced to the two conformational changes which distinguish the intermediate from the fully activated conformations: helix D elongation and β-sheet A contraction.

Thus we are now in a stronger position to address the questions raised earlier: What is the conformational change which creates the high-affinity state, and how is the remote binding of heparin translated into β-sheet A contraction? First, as mentioned above, since there are no differences in the interaction between the pentasaccharide and the intermediate or the fully activated forms of antithrombin, an improved interaction interface cannot be the reason behind the high-affinity state. What accounts for the change in global free energy will thus be either helix D elongation or sheet A contraction or both. Both hydrogen bond enthalpy and reactive center loop entropy terms should favor the five-stranded, fully activated conformation. In addition to the predictable energetic effects is the more opaque contribution of packing, which may also be improved in the activated state. Although the energetic contributions are difficult to surmise from the structure, the conformational change to the high-affinity form is characterized kinetically by a multiple order of magnitude drop in the rate of complex dissociation, k_{off}. Since k_{off} is indistinguishable from the reverse conformational change step, k_{-2}, it can be concluded that the major effect of the conformational change from the intermediate

to the fully activated state of antithrombin is the locking of the contracted five-stranded β-sheet A form. So which of the two conformational events, helix D elongation or sheet A contraction, is the locking event? The observations that the latent form bound to the pentasaccharide lacks helix D elongation (*4*) and that a proline mutation in the elongated portion of helix D (K133P) (*32*) increases k_{-2} implicate helix D elongation as the locking event.

The C-terminal portion of helix D is not traceable in the electron density of the intermediate structure between Lys133 and Ser137, implying disorder. However, when the fully activated structure is superimposed on the intermediate structure, it is clear that, for steric reasons, helix D cannot be elongated in the absence of expulsion of the reactive center loop and β-sheet A contraction (Figure 3c). Conversely, sheet A, once five-stranded, cannot revert to the six-stranded native state without causing the unraveling of the C-terminus of helix D. Evidence that an elongated helix D cannot exist in the context of a six-stranded β-sheet A is provided by its conspicuous absence from all antithrombin forms crystallized except the fully activated state. Similarly, one would predict that helix D elongation cannot precede, and thus must follow, β-sheet A contraction in the activation pathway. This is supported by the K133P mutant, which had little effect on the forward conformational change step k_2 and only affected k_{-2}, and the β-isoform of antithrombin (lacking glycosylation at Asn135), which binds heparin more tightly primarily due to an effect on k_{-2} (*15*).

Helix D elongation and β-sheet A contraction are thus linked events, which also link conformational change in the heparin binding region to the contraction of β-sheet A. Although this observation suggests a mechanism of propagation of conformational change, it does not account for the conformational changes which have already taken place in the intermediate form. In the seminal paper by van Boeckel and colleagues in 1994 (*33*) a mechanism of heparin activation was proposed on the basis of the structure of native antithrombin, biochemical observation, and modeling. The authors predicted that heparin binding would lead to a contraction of β-sheet A which would cause the expulsion of the reactive center loop. Our structure of the intermediate form confirms this prediction in part, since β-sheet A in the intermediate form has contracted by four hydrogen bonds. It is possible that this initial contraction event renders antithrombin competent of full β-sheet A contraction and favors the expulsion of the hinge region.

A modified mechanism can now be proposed for the kinetic pathway of heparin activation of antithrombin. As illustrated in the video, native antithrombin binds weakly to heparin until the pentasaccharide sequence is encountered, at which point a conformational change takes place which forms the pentasaccharide binding site. This intermediate structure has undergone partial contraction of β-sheet A and all other heparin-induced conformational changes save helix D expansion and hinge region expulsion. β-Sheet expulsion is more readily accessible from the intermediate conformation, and once it occurs, helix D elongation serves to lock antithrombin in the five-stranded, fully activated state.

ACKNOWLEDGMENT

The authors thank Trevor P. Baglin, Robin W. Carrell, and Randy Read for reading the manuscript.

SUPPORTING INFORMATION AVAILABLE

The figure shows the electron density generated using molecular replacement solutions for pentasaccharide-bound (1e03) and native (1e05) antithrombin, and the video shows antithrombin binding to a specific heparin pentasaccharide by a three-step mechanism. This material is available free of charge via the Internet at http://pubs.acs.org.

REFERENCES

1. Thunberg, L., Backstrom, G., and Lindahl, U. (1982) *Carbohydr. Res. 100*, 393.
2. Choay, J., Petitou, M., Lormeau, J. C., Sinay, P., Casu, B., and Gatti, G. (1983) *Biochem. Biophys. Res. Commun. 116*, 492.
3. Olson, S., Bjork, I., and Bock, S. (2002) *Trends Cardiovasc. Med. 12*, 198.
4. Jin, L., Abrahams, J. P., Skinner, R., Petitou, M., Pike, R. N., and Carrell, R. W. (1997) *Proc. Natl. Acad. Sci. U.S.A. 94*, 14683.
5. Bjork, I., and Olson, S. T. (1997) *Adv. Exp. Med. Biol. 425*, 17.
6. Olson, S. T., Srinivasan, K. R., Bjork, I., and Shore, J. D. (1981) *J. Biol. Chem. 256*, 11073.
7. Huntington, J. A., and Carrell, R. W. (2001) *Sci. Prog. 84*, 125.
8. Schreuder, H. A., de Boer, B., Dijkema, R., Mulders, J., Theunissen, H. J., Grootenhuis, P. D., and Hol, W. G. (1994) *Nat. Struct. Biol. 1*, 48.
9. Carrell, R. W., Stein, P. E., Fermi, G., and Wardell, M. R. (1994) *Structure 2*, 257.
10. Whisstock, J. C., Pike, R. N., Jin, L., Skinner, R., Pei, X. Y., Carrell, R. W., and Lesk, A. M. (2000) *J. Mol. Biol. 301*, 1287.
11. Meagher, J. L., Beechem, J. M., Olson, S. T., and Gettins, P. G. (1998) *J. Biol. Chem. 273*, 23283.
12. Zhou, A., Huntington, J. A., and Carrell, R. W. (1999) *Blood 94*, 3388.
13. Rosenfeld, L., and Danishefsky, I. (1984) *Arch. Biochem. Biophys. 229*, 359.
14. Picard, V., Ersdal-Badju, E., and Bock, S. C. (1995) *Biochemistry 34*, 8433.
15. Turk, B., Brieditis, I., Bock, S. C., Olson, S. T., and Bjork, I. (1997) *Biochemistry 36*, 6682.
16. Zhou, A., Stein, P. E., Huntington, J. A., and Carrell, R. W. (2003) *J. Biol. Chem. 278*, 15116.
17. Leslie, A. W. G. (1992) *Joint CCP4 and ESF-EACMB Newsletter on Protein Crystallography*, Daresbury Laboratory, Warrington, U.K.
18. Vagin, A., and Teplyakov, A. (2000) *Acta Crystallogr., Sect. D: Biol. Crystallogr. 56* (Part 12), 1622.
19. McRee, D. E. (1992) *J. Mol. Graphics 10*, 44.
20. Brunger, A. T., Adams, P. D., Clore, G. M., Delano, W. L., Gros, P., GrosseKunstleve, R. W., Jiang, J. S., Kuszewski, J., Nilges, M., Pannu, N. S., Read, R. J., Rice, L. M., Simonson, T., and Warren, G. L. (1998) *Acta Crystallogr. D54*, 905.
21. McCoy, A. J., Pei, X. Y., Skinner, R., Abrahams, J. P., and Carrell, R. W. (2003) *J. Mol. Biol. 326*, 823.
22. Kraulis, P. J. (1991) *J. Appl. Crystallogr. 24*, 946.
23. Esnouf, R. M. (1997) *J. Mol. Graphics Modelling 15*, 132.
24. Merritt, E. A., and Murphy, M. E. P. (1994) *Acta Crystallogr. D50*, 869.
25. Elliott, P. R., Lomas, D. A., Carrell, R. W., and Abrahams, J. P. (1996) *Nat. Struct. Biol. 3*, 676.
26. Sharp, A. M., Stein, P. E., Pannu, N. S., Carrell, R. W., Berkenpas, M. B., Ginsburg, D., Lawrence, D. A., and Read, R. J. (1999) *Struct. Folding Des. 7*, 111.
27. Wei, A., Rubin, H., Cooperman, B. S., and Christianson, D. W. (1994) *Nat. Struct. Biol.*, 251.
28. Li, J., Wang, Z., Canagarajah, B., Jiang, H., Kanost, M., and Goldsmith, E. J. (1999) *Struct. Folding Des. 7*, 103.
29. Huntington, J. A., McCoy, A., Belzar, K. J., Pei, X. Y., Gettins, P. G., and Carrell, R. W. (2000) *J. Biol. Chem. 275*, 15377.
30. Huntington, J. A., Olson, S. T., Fan, B., and Gettins, P. G. (1996) *Biochemistry 35*, 8495.
31. Huntington, J. A., and Gettins, P. G. (1998) *Biochemistry 37*, 3272.
32. Belzar, K. J., Zhou, A., Carrell, R. W., Gettins, P. G., and Huntington, J. A. (2002) *J. Biol. Chem. 277*, 8551.
33. van Boeckel, C. A., Grootenhuis, P. D., and Visser, A. (1994) *Nat. Struct. Biol. 1*, 423.

BI034524Y